

## NEUROSYSTEMS

# Comparison of visual receptive fields in the dorsolateral prefrontal cortex and ventral intraparietal area in macaques

Pooja Viswanathan and Andreas Nieder 

Animal Physiology, Institute of Neurobiology, University of Tübingen, Auf der Morgenstelle 28, 72076 Tübingen, Germany

**Keywords:** PFC, primate, receptive field, single-unit recording, VIP

## Abstract

The concept of receptive field (RF) describes the responsiveness of neurons to sensory space. Neurons in the primate association cortices have long been known to be spatially selective but a detailed characterisation and direct comparison of RFs between frontal and parietal association cortices are missing. We sampled the RFs of a large number of neurons from two interconnected areas of the frontal and parietal lobes, the dorsolateral prefrontal cortex (dlPFC) and ventral intraparietal area (VIP), of rhesus monkeys by systematically presenting a moving bar during passive fixation. We found that more than half of neurons in both areas showed spatial selectivity. Single neurons in both areas could be assigned to five classes according to the spatial response patterns: few non-uniform RFs with multiple discrete response maxima could be dissociated from the vast majority of uniform RFs showing a single maximum; the latter were further classified into full-field and confined foveal, contralateral and ipsilateral RFs. Neurons in dlPFC showed a preference for the contralateral visual space and collectively encoded the contralateral visual hemifield. In contrast, VIP neurons preferred central locations, predominantly covering the foveal visual space. Putative pyramidal cells with broad-spiking waveforms in PFC had smaller RFs than putative interneurons showing narrow-spiking waveforms, but distributed similarly across the visual field. In VIP, however, both putative pyramidal cells and interneurons had similar RFs at similar eccentricities. We provide a first, thorough characterisation of visual RFs in two reciprocally connected areas of a fronto-parietal cortical network.

## Introduction

The region of sensory space within which a stimulus can modulate a neuron's response circumscribes the receptive field (RF) of that neuron (Hubel & Wiesel, 1962). For neurons in primary sensory areas, this region is described quite simply by the sensory receptors that relay information to it. Higher association areas that receive information from lower areas are able to integrate information across various stimulus components and can, thus, display a range of complexity in their RFs (Blatt *et al.*, 1990; Avillac *et al.*, 2005). However, neurons in higher association cortices, such as areas in the dorsolateral prefrontal cortex (dlPFC) and in the posterior parietal cortex (PPC), are not often characterised by their receptive field structure as they are in primary sensory cortices (Alonso, 2002; Solomon *et al.*, 2002;

Swadlow & Gusev, 2002; Yoshor *et al.*, 2007; Veit *et al.*, 2014). Most studies map either dlPFC or PPC RFs coarsely and in isolation from one another to aid presentation of stimuli that require active discrimination or subsequent comparison.

Ventral intraparietal area (VIP) of the PPC is located in the fundus of the intraparietal sulcus (IPS; Colby *et al.*, 1993). It receives visual information primarily from the middle temporal (MT) area and dense multi-modal input from its surrounding areas (Lewis & Van Essen, 2000). Consequently, VIP neurons respond to visual, auditory, tactile and vestibular information (Bremmer *et al.*, 2002; Avillac *et al.*, 2005; Schlack *et al.*, 2005). Single neurons in VIP have a sophisticated multi-modal representation of objects in space using different reference frames (Avillac *et al.*, 2007; Zhang & Britten, 2011). During steady fixation, these reference frames converge, allowing for different sensory modalities to be represented in a single frame. During movement, these reference frames are sometimes found to shift from eye-centred (Chen *et al.*, 2014) to head-centred representations (Duhamel *et al.*, 1997), possibly enabling spatial transformations during movement (Bremmer, 2011).

Neurons in the dlPFC exhibit visual RFs (Mikami *et al.*, 1982; Suzuki & Azuma, 1983) and also show multi-sensory responses (Suzuki, 1985; Romo *et al.*, 1999; Sugihara *et al.*, 2006; Nieder, 2012; Wang *et al.*, 2015). Even the hallmark feature of prefrontal

*Correspondence:* Andreas Nieder, as above.

E-mail: andreas.nieder@uni-tuebingen.de

Received 27 July 2017, revised 3 October 2017, accepted 5 October 2017

Edited by Helen Barbas

Reviewed by Christos Constantinidis, Wake Forest University School of Medicine, USA; and Maria Medalla, Boston University, USA

The associated peer review process communications can be found in the online version of this article.

neurons: working memory (Fuster & Alexander, 1971; Fuster & Bauer, 1974) has a spatial component. Neurons have been described as having 'memory fields' (Funahashi & Bruce, 1989) which circumscribe the area of increased delay period activity of a certain neuron to a preferred object when it is presented in a specific part of the visual field (Rainer *et al.*, 1998a). Thus, while retaining the representation of an object, they additionally retain its location.

Examining RFs in both PFC and PPC together is motivated by the finding that areas of the PPC and dIPFC are anatomically and functionally connected (Schwartz & Goldman-Rakic, 1984; Pandya & Yeterian, 1991; Lewis & Van Essen, 2000). For example, temporary inactivation of one region changes the response properties of neurons in the other (Quintana & Fuster, 1999; Chafee & Goldman-Rakic, 2000). This suggests a close functional interdependence between the two regions that form association networks. To learn about their respective contributions, neurons in the dIPFC and intraparietal sulcus (IPS) have been studied together as part of a fronto-parietal network (Buschman & Miller, 2007; Swaminathan & Freedman, 2012; Crowe *et al.*, 2013). The fronto-parietal network involving the dIPFC and the ventral intraparietal area (VIP) is specifically implicated in the magnitude system in primates (Nieder & Miller, 2004; Tudusciuc & Nieder, 2009; Vallentin *et al.*, 2012; Viswanathan & Nieder, 2013, 2015; Nieder, 2016). However, surprisingly little is known about the RFs in these areas, how they compare to the visual cortex, and how they compare with each other. We have recently found that the spatiotopic organisation of early visual cortices is no longer retained in these higher association areas (Viswanathan & Nieder, 2017), thus, motivating the question whether the RFs in these association areas display much non-uniformity.

Here, we investigate the spatial selectivity of neurons in the dIPFC and VIP with a moving bar stimulus shown at different locations on the screen while the monkeys passively fixate a central fixation spot. We found that a large number of neurons selectively responded to the object at various positions of the screen, and we created receptive field maps for these neurons. We characterise the different types of receptive fields in the respective brain areas based on their structure, location and size and the different types of neurons based on their extracellular waveforms. These results provide the first and largest detailed characterisation of PFC receptive fields, in direct comparison with VIP receptive fields acquired simultaneously.

## Materials and methods

### *Subjects and experimental setup*

Two male rhesus monkeys (*Macaca mulatta*) weighing between 5.5 and 6.3 kg were used for this experiment. All experimental procedures were in accordance with the guidelines for animal experimentation approved by the national authority, the Regierungspräsidentium Tübingen, Germany. The monkeys were socially housed, in groups of 2 to 4. During experiments, the monkeys sat in primate chairs within experimental chambers and received fluid rewards. The monkeys were positioned 57 cm from a 15" flat screen monitor with a resolution of 1024 by 768 pixels and a refresh rate of 75 Hz. We used the NIMH Cortex programme to present the stimuli, monitor the behaviour and collect behavioural data. Cortex communicated with an infrared tracking system (ISCAN, Cambridge, MA, USA) to monitor the monkeys' eyes and collect eye-tracking data. All data analysis was performed using custom-written scripts in the MATLAB computational environment (Mathworks).

### *Surgery and electrophysiological recordings*

First, the monkeys were implanted with a head bolt to allow monitoring of eye movements during the task. After training on the behavioural tasks, we implanted recording chambers over the right dorsolateral prefrontal cortex, centred on the principal sulcus, and the right intraparietal sulcus guided by anatomical MRI and stereotaxic measurements (Figs 1A and 3). The surgical procedures were performed under sterile conditions. Anaesthesia was induced by ketamine hydrochloride (10 mg/kg) and xylazine (5 mg/kg). For maintenance of anaesthesia, we used nitrous oxide and isoflurane, monitoring the levels and vital signs during the procedure. The monkeys received post-surgical analgesics and antibiotics. The recording chambers were sealed with sterile caps and cleaned regularly with antiseptic washes.

For the recordings, we used arrays of eight glass-coated tungsten microelectrodes (Alpha Omega Ltd., Israel) attached to screw micro-drives in a grid with 1 mm spacing. For PFC recordings, we recorded from neurons as soon as we entered cortex (Fig. 3A and B). For VIP recordings, we lowered the electrodes to depths of 9 to 14 mm from the cortical surface (Fig. 3C and D). The electrophysiological signals were amplified, filtered and waveforms of the actions potentials sampled at 40 kHz from each electrode were stored (Plexon Systems, USA). Single units were sorted offline based on waveform characteristics (Offline Sorter, Plexon Systems). In all, we recorded 1186 PFC neurons and 944 VIP neurons.

### *Behavioural task*

During the receptive field measurements, the monkeys performed a passive fixation task. They were rewarded for maintaining fixation on a central white square ( $0.10^\circ \times 0.10^\circ$  of visual angle or dva) while a grey moving bar ( $3^\circ \times 0.20^\circ$ ) appeared on the screen at five successive positions on the screen (Fig. 1B) in each trial. The positions were selected pseudo randomly from a 10 (horizontal)  $\times$  8 (vertical) grid of positions. The moving bar covered each position for 1000 ms divided between 2 orientations and 2 directions of movement. First, the bar was oriented vertically moving left to right ( $0^\circ$  for 250 ms), right to left ( $180^\circ$  for 250 ms), then oriented horizontally moving up ( $90^\circ$  for 250 ms), moving down ( $270^\circ$  for 250 ms). The bar moved at a constant speed of  $8^\circ$  per second and covered a distance of  $2^\circ$  per sweep. The grid of locations thus covered the entire screen, that is  $30.5^\circ \times 23^\circ$  of central vision. The monkeys were rewarded for successfully fixating the whole trial. Receptive field measurement blocks were interleaved with delayed match-to-sample task blocks (Viswanathan & Nieder, 2013, 2015). Each recording session could yield up to 4 RF mapping blocks.

### *Spatial selectivity*

Of the neurons we recorded, many of them responded to the spatial position of the moving bar even as the monkeys fixated the central fixation spot. To ascertain their receptive fields, we first tested the neurons for spatially selective responses. We analysed the responses of all the neurons in the 1000 ms period that each position was tested. To account for well-known differences in response latencies in these two areas (Nieder & Miller, 2004; Viswanathan & Nieder, 2013), we delayed the onset of the analysis window for VIP neurons by 50 ms and for PFC neurons by 100 ms. We calculated a 3-way ANOVA on firing rates calculated in a 250 ms period corresponding to the duration of a single bar sweep, with position, movement direction and orientation of the bar as factors (Rainer *et al.*, 1998a; Romero & Janssen, 2016). The movement direction was applied as a nested variable of orientation. We down-sampled the screen into five

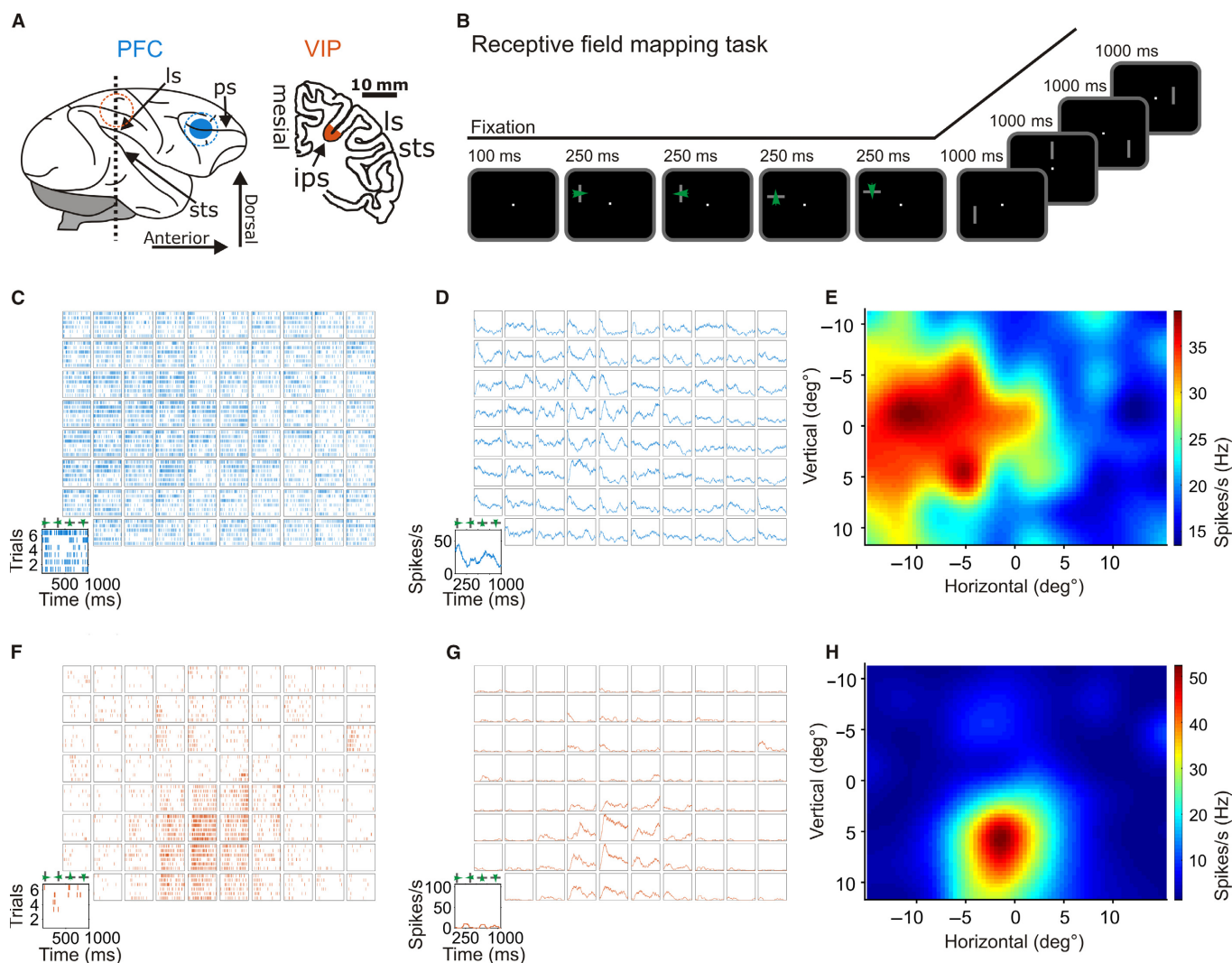


**FIG. 1.** Receptive field mapping. (A) Positions of recording sites in the dorsolateral prefrontal cortex (dIPFC, cyan) shown in the lateral view of a rhesus monkey brain and the ventral intraparietal area (VIP, orange) in the depth of the intraparietal sulcus (IPS) depicted in a coronal section of the sulcus. LS, lateral sulcus; PS, principal sulcus; STS, superior temporal sulcus. (B) The receptive field mapping task began with a short fixation period of 100 ms. Following this, a moving bar was shown in five successive positions on the screen while the monkeys continued to fixate centrally. The screen was divided into 80 locations sampled over multiple trials. Each trial of successful fixation was positively reinforced. (C) The trial-by-trial activity of an example PFC neuron is shown as a raster plot. Each subplot has trials plotted against time during the 1000 ms of stimulus presentation at that location of the screen. Each individual line shows an action potential fired by the neuron. (D) The trial-averaged activity of the same neuron is shown for every location, the average discharge rate against time. (E) Next, the activity at each location is averaged in time to create a raw RF map. The raw RF map is then linearly interpolated in both dimensions and smoothed with a 2D Gaussian to create a high-resolution RF map. The discharge rate is indicated by the warmth of the colour. (F) Dot raster plot for an example VIP neuron. (G) Peri-stimulus time histogram (PSTH) of the same neuron for every stimulus location. (H) High-resolution RF map for the VIP neuron. [Colour figure can be viewed at [wileyonlinelibrary.com](http://wileyonlinelibrary.com)].

zones (top left, top right, bottom left, bottom right and centre) to limit the levels of the variable position to 5, comparable to four directions and two orientations. We tested every neuron with a minimum of two trials per location (859 PFC neurons and 693 VIP neurons) and evaluated the ANOVA results with an alpha of 0.05.

We created raw RF maps for every neuron with  $P < 0.05$  by averaging the responses for each position over the 1000 ms period. To view responses at a higher resolution, we linearly interpolated the raw RF maps by 3-fold in both spatial dimensions and smoothed them with a 2D Gaussian kernel of 2 dva. We conducted a further cross-validation using these maps to confirm robust spatial selectivity. We created two separate RF maps for each neuron; one from the first half of RF trials and another from the second half of trials. We calculated a 2D cross-correlation between the two maps created

for each neuron and compared this against a distribution of 2D cross-correlations calculated from 1000 shuffles of each half map.

$$r = \frac{\sum_h \sum_v (\text{Half 1} - \overline{\text{Half 1}})(\text{Half 2} - \overline{\text{Half 2}})}{\sqrt{(\sum_h \sum_v (\text{Half 1} - \overline{\text{Half 1}})^2)(\sum_h \sum_v (\text{Half 2} - \overline{\text{Half 2}})^2)}$$

where Half1 is the map created from the first half of trials and Half2 is the map created from the second half of trials. The means of the maps are subtracted before summing them over the horizontal,  $h$  and vertical,  $v$  dimensions. Only if the true correlation across halves of trials lay above the 95th percentile of the distribution of surrogate correlations (one-tailed,  $P < 0.05$ ), we accepted the neuron and its RF map into further analysis.

### Strength of spatial selectivity

Using these spatially selective neurons, we created average maps for each area. We also created normalised maps for each neuron by dividing the RF map by the maximum of each map. We then averaged the normalised maps of all PFC neurons and all VIP neurons (Rainer *et al.*, 1998a) to quantify the strength of spatial modulation in each area.

We calculated an omega-squared ( $\omega^2$ ) value for each neuron. This estimates how much of the variance in the trial-by-trial firing rates could be explained by the position of the bar stimuli on the screen. It is derived from a one-way ANOVA with the factor position over the entire 1000 ms of stimulation at each position.

A selectivity index (SI) helped to compare the response of each neuron within its RF and outside its RF and was calculated using:

$$SI = (FR_{\max} - FR_{\min}) / (FR_{\max} + FR_{\min})$$

where  $FR_{\max}$  is the maximum firing rate of the neuron and  $FR_{\min}$  is the minimum firing rate of the neuron. The SI can have values between 0 and 1. Values close to 1 indicate high spatial selectivity and very low responses to areas outside the RF.

### Characterisation of receptive fields

We found five possible classes of receptive fields which could be separated based on the uniformity, size and location of responses. To separate them in an unbiased manner, we normalised each map to the maximum across positions for that neuron. Some neurons showed multiple local maxima of more than 9°, and we characterised these as non-uniform (threshold = 98% of maximum). For the remaining neurons, the receptive field could simply be described as the contiguous area that activated the neuron to more than half of its maximal response (Rainer *et al.*, 1998a; Romero & Janssen, 2016). However, a subset of these neurons had receptive fields that spanned more than 75% of the screen showing very small local minima. We considered these neurons to be full-field neurons. We classified the remaining neurons with confined fields according to where their maxima lay on the horizontal axis of the visual field, contralateral visual field, foveal or ipsilateral visual field. We confirmed that classifying them according to the centre of mass, that is the geometric centre weighted by the activity, yielded quantitatively similar results as classifying them using the location of the maxima.

To reliably calculate RF eccentricities, we limited our analysis to neurons whose receptive fields were uniform, but not full-field. We calculated the Euclidian distance of the RF maxima from the central fixation point as the RF eccentricity. Calculating the Euclidian distance between the centre of mass of the RF and the fixation point yielded similar results. Our calculation of RF sizes further took into account that not all RFs were within the screen. Some neurons seemed to have RFs that began at the edges of the screen and possibly extended to visual space outside it. So, we limited our calculation of RF sizes to neurons with screen-limited RFs. We did not fit a shape to the receptive field to allow for complex, non-Gaussian shapes as can be expected from such associative areas. The RF of the neuron was the area of the map that displayed activity >0.5 of maximal response. The RF size was thus the square root of the total degrees of visual angle it spanned.

We use the Kolmogorov–Smirnov test to compare the distributions of RF eccentricity and size. We use the non-parametric Mann–Whitney *U*-test to compare the central tendencies (the medians) of

RF eccentricity and size across areas and judged the results with an alpha of 0.05. All tests, unless specified, are two-tailed.

### Receptive fields of neuronal classes

We classified the recorded single units into putatively interneuron (narrow-spiking, NS) and pyramidal (broad-spiking, BS) neuronal classes based on their extracellular waveforms (Diester & Nieder, 2008; Viswanathan & Nieder, 2015). We saved the template waveforms for each single unit but only classified those that had a classic downward deflection upon reaching threshold followed by an upward peak (1951/2130 neurons). The troughs occurred between 200 to 400  $\mu$ s and the crests only after 300  $\mu$ s. We normalised the waveforms to the difference between the maximum amplitude and the minimum amplitude and aligned them to their troughs. We then entered the waveforms through a linear classifier (*k*-means;  $k = 2$ , squared Euclidian distance) to cluster the cells into two categories: narrow-spiking (NS) and broad-spiking (BS) such that on average, the units with smaller widths constituted the narrow-spiking cluster (537 neurons) and those with the larger widths constituted the broad-spiking cluster (1414 neurons) (Fig. 8A and B).

## Results

### Single neurons in PFC and VIP exhibit visual RFs

We simultaneously recorded single-cell activity in the dorsolateral prefrontal cortex (dIPFC) around the principal sulcus (PS) and in the ventral intraparietal area (VIP) in depths of the intraparietal sulcus (IPS). The recordings were made in the right hemisphere of two monkeys performing a simple passive fixation task (Fig. 1A). While the monkeys fixated a central fixation target, a moving bar was presented at various locations of the screen (Fig. 1B). In response to this simple stimulus, many dIPFC and VIP neurons fired action potentials when the stimulus was at certain positions in the visual field. We collected firing rates for each of the 80 positions investigated over multiple trials (Fig. 1C and F). Activity was then averaged across trials (Fig. 1D and G) to create receptive field (RF) maps (Fig. 1E and H) for every spatially selective neuron. Figure 1C–E displays a dIPFC neuron with selective increases in firing rates whenever the bar was presented to the left of the fixation target, that is this neuron had a large RF in the contralateral visual hemi-field because all recordings were made from the right hemisphere. In contrast, a representative VIP neuron (Fig. 1F–H) only responded to bars in a very confined visual region about 5 deg below and 2 deg right from the fixation target, or visual fovea, respectively. This resulted in a small and strongly spatially selective RF in this VIP neuron.

We statistically tested neuronal selectivity to the moving bar by calculating a 3-way ANOVA with ‘position’, ‘movement direction’ and ‘orientation’ as main factors. The highest proportion of neurons was selective to bar position than the other main factors ( $P < 0.05$ ). In the dIPFC, 64% (545/859) of the neurons showed a stimulus position effect. In VIP, 69% (480/693) of all neurons were spatially tuned. Neurons in both areas were also tuned to the movement direction and orientation of the bar. In dIPFC, 39% (332/859) and 44% (374/859) neurons were selective for direction and orientation, respectively. In VIP, 46% (317/693) and 44% (307/693) of neurons were selectively tuned to the direction and orientation. We cross-validated the RFs of spatially tuned neurons to ensure that their responses were robust and stable in time (Viswanathan & Nieder, 2017). To that aim, we created two separate RF maps for every

neuron from half the trials each and calculated the 2D correlation coefficient between them. We compared the neuron's true correlation coefficient against a distribution of coefficients obtained from correlating shuffled surrogates (one-tailed,  $P < 0.05$ ). Half of the dIPFC neurons (50%, 425/859) passed both the ANOVA test and the 2D correlation-criterion and henceforth constituted the population of dIPFC neurons with a visual RFs (Fig. 2A). The same criterion applied to the VIP resulted in 57% (396/693) of VIP neurons showing a robust visual RF (Fig. 2B). Only these neurons and their RFs were used in further analyses. The proportion of neurons showing visual RFs was higher in VIP compared to dIPFC ( $\chi^2 = 9.05$ ,  $P = 0.003$ ).

To find out whether the population of neurons in PFC and VIP cover the visual field evenly or rather show spatial preferences, we examined the distribution of the RFs across the visual fields. We found that most PFC neurons had their RF maxima in the visual hemi-field contralateral to the recorded hemisphere, i.e. covered predominantly the left visual hemi-field for recording sites in the right hemisphere (Fig. 2C). The largest number of neurons ( $n = 132$ ) in PFC had their RFs between  $-10^\circ$  and  $-17^\circ$  on the horizontal axis. In VIP, on the other hand, most neurons had their RFs clustered around the fovea with a bias towards the contralateral hemi-field (Fig. 2D). The RFs ( $n = 154$ ) were maximally clustered between  $-3^\circ$  and  $-10^\circ$  on the horizontal axis.

We reconstructed the recording sites and examined the topographic layout of RFs (Fig. 3). In PFC, our recordings sites mostly spanned the dorsal and ventral parts of the prearcuate gyrus in both monkeys (Fig. 3A and B). We normalised each RF map to its maximum and averaged all such maps obtained at each recording site. We did not observe a topographic difference in the kinds of RFs. In the VIP, our recordings were in the depth of the intraparietal sulcus, starting at 9 mm from the cortical surface and exploring up to 14 mm into the banks of the IPS in both monkeys (Fig. 3C and D). The averaged maps at each site again show no topographic organisation.

To visualise how the entire population of neurons in the respective brain areas would encode the visual space as a whole, we created average RF maps. First, we constructed such maps by

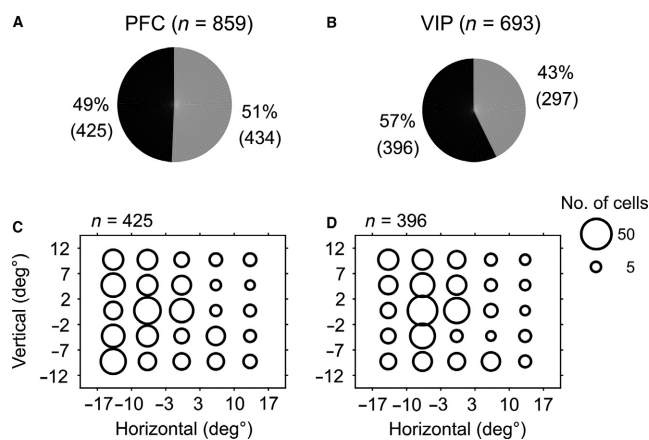


FIG. 2. Spatially selective population and the spatial distribution of RFs. (A) Proportion of PFC neurons that exhibit a spatial RF; 49% of 859 neurons against the non-selective population depicted in grey. (B) Proportion of VIP neurons that exhibit a spatial RF; 57% of 693 neurons against the non-selective population. (C) Distribution of the location of PFC RF maxima across the screen. The size of the circle reflects the number of neurons with their maxima at that location. (D) the same as C for VIP neurons. PFC shows a contralateral bias.

averaging the absolute firing rates of individual neurons, which emphasised the contribution of the neurons with strong spatial firing rate modulation. The population of dIPFC neurons responded more strongly to the contralateral visual hemisphere with an emphasis on the lower quadrant (Fig. 4A). In contrast, VIP neurons displayed strongest responses around the central fixation area with a bias towards the contralateral hemi-field (Fig. 4B).

The average RF maps might be dominated by neurons with particularly high firing rates. In fact, VIP neurons displayed on average higher firing rates than dIPFC neurons (mean<sub>PFC</sub> = 5.1 Hz, mean<sub>VIP</sub> = 6.8 Hz; Mann–Whitney  $U$ -test,  $Z = -2.8$ ,  $P = 0.005$ ). To weigh the contribution of individual neurons equally and irrespective of their absolute firing rates, we constructed normalised average RF maps for dIPFC and VIP by normalising the response of each neuron relative to its maximum activity. After normalisation, the population RF map in VIP still shows a predominantly foveal focus with a bias towards the contralateral hemi-field (Fig. 4D). In the PFC, however, the representation of visual space (based on spatial activity modulation) became much more evenly distributed across the entire visual field, with a mild over-representation of the contralateral hemi-field (Fig. 4C). We quantified the strength of spatial modulation in the population of selective neurons by calculating the  $\sigma^2$  value. The measure describes how much of the variance in the firing rate of a neuron was explained by the explanatory variable, stimulus location. On average, 9% of the variance in PFC neuronal activity was explained by the spatial position while as much as 11% of the variance in VIP neuronal activity was explained by bar location. This difference in  $\sigma^2$  was highly significant (Mann–Whitney  $U$ -test,  $Z = -4.2$ ,  $P < 0.0001$ ). A comparison of modulation of firing rates by the RF showed that VIP neurons had slightly higher selectivity indices than PFC neurons (median<sub>PFC</sub> = 0.889, median<sub>VIP</sub> = 0.894; Mann–Whitney  $U$ -test,  $Z = -2.16$ ,  $P = 0.03$ ).

### Classes of receptive fields

The detailed RF maps we created helped to characterise the selective responses of the neurons and examine the structures of RFs. The RFs could be assigned to five classes (Romero & Janssen, 2016) in both dIPFC and VIP (Fig. 5). We found 44 dIPFC and 38 VIP neurons that had multiple discrete maxima and classified them as non-uniform RFs (Fig. 5A and B). The rest of the neurons could be described as uniform RFs. However, a small proportion of neurons, 23 PFC neurons and 34 VIP neurons, respectively, showed full-field activity with the RF covering more than 75% of the visual field on the screen (Fig. 5C and D). The frequencies of these classes of RFs were indistinguishable between areas ( $\chi^2 = 2.39$ ,  $P = 0.12$ ). The rest of the neurons had uniform, confined receptive fields located either in the contralateral (i.e. left) visual field (Fig. 5E and F), foveally (central) (Fig. 5G and H) or in the ipsilateral (i.e. right) visual field (Fig. 5I and J). The frequency counts of the various types of RFs are shown in Fig. 6A and B for areas dIPFC and VIP, respectively. Note that dIPFC exhibited a much higher frequency of contralateral RFs than VIP ( $\chi^2 = 17.22$ ,  $P < 0.0001$ ). In contrast, VIP contained a higher number of neurons with foveal RFs ( $\chi^2 = 21.17$ ,  $P < 0.0001$ ). The frequency of ipsilateral RFs between the two areas, however, were indistinguishable ( $\chi^2 = 0.92$ ,  $P = 0.34$ ).

### Receptive field eccentricity and size

A characteristic aspect of receptive fields is their eccentricity from the fovea, measured as the Euclidean distance between the RF maxima and the centre. When we estimated this for the neurons with

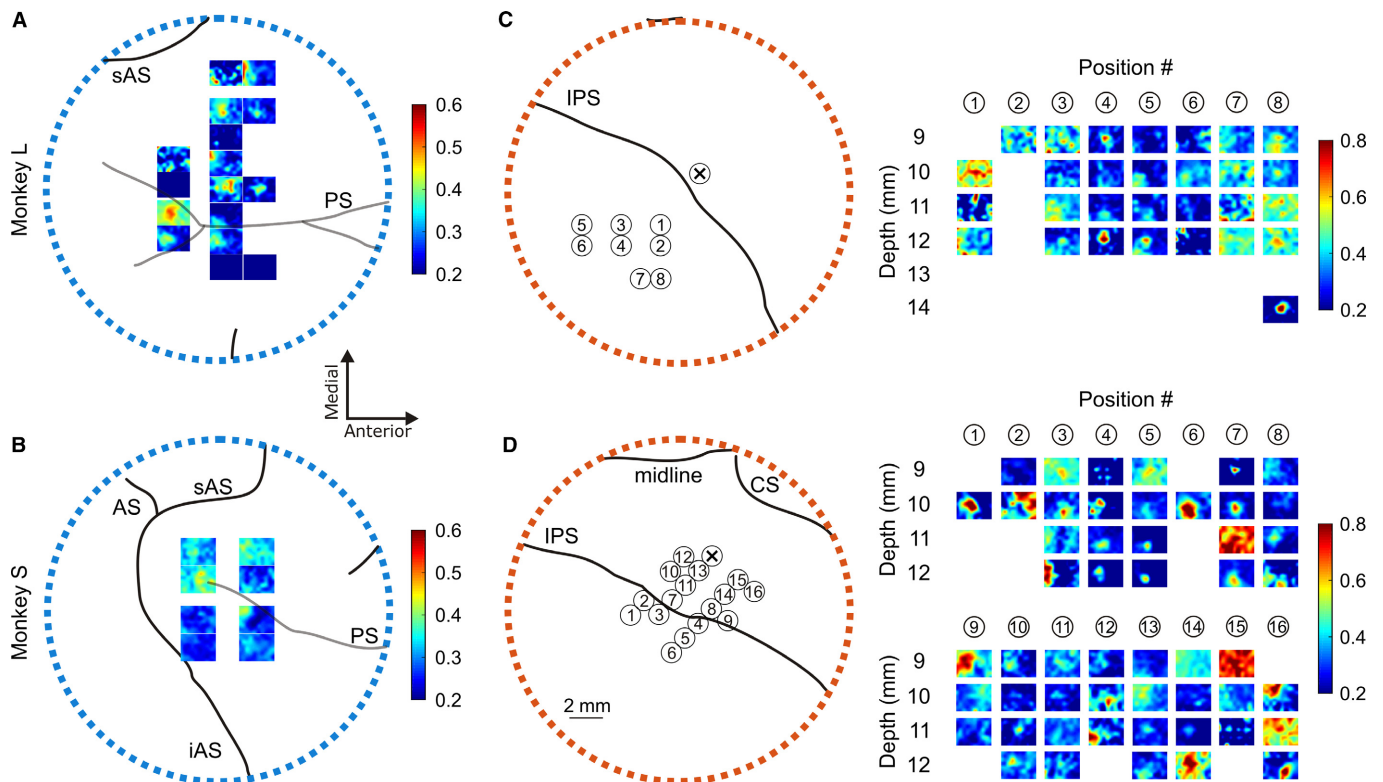


FIG. 3. Recording sites in the dIPFC and VIP. (A) RF maps from the individual recording sites around the principal sulcus of monkey L. All the RFs recorded at each site are normalised individually and then averaged. AS, arcuate sulcus; sAS, superior arcuate sulcus; iAS, inferior arcuate sulcus; PS, principal sulcus. (B) Averaged RF maps from the individual recording sites in monkey S. (C) Recording sites in area VIP of monkey L on the banks of the intraparietal sulcus, labelled and numbered, *left panel*. IPS, intraparietal sulcus; CS, central sulcus. RF maps from each site and at the indicated depth from the cortical surface, *right panel*. (D) same as C for recording sites in monkey S. Colour bars on the right show the normalised firing rate. [Colour figure can be viewed at [wileyonlinelibrary.com](http://wileyonlinelibrary.com)].

uniform, confined RFs, we found uniformly-distributed RF eccentricities covering the entire monitor space between  $0.1^\circ$  and  $18^\circ$  (Fig. 7A and B). With a median RF eccentricity of  $12^\circ$ , neurons in dIPFC exhibited more eccentric RFs than VIP neurons with a median of  $9.6^\circ$  (Mann–Whitney *U*-test,  $Z = 3.49$ ,  $P < 0.001$ ).

We measured the receptive field sizes of the neurons whose RFs were confined. Non-uniform or uniform full-field RFs were therefore excluded. Further, 80% (286/358) PFC neurons and 74% (241/324) VIP neurons had RFs that were confined but extended beyond the borders of our measurement. We excluded such neurons to limit our calculation of RF sizes to neurons whose fields were limited to the screen. The RF size of such screen-limited neurons was the square root of the area with half-max activity. For both dIPFC and VIP, this yielded RF sizes between  $3.7^\circ$  and  $13.8^\circ$  (Fig. 7C and D). The distributions of RF sizes, however, were significantly different in the two areas (Kolmogorov–Smirnov test for unequal cdfs = 0.29,  $P = 0.003$ ), with larger RF sizes in VIP than those in dIPFC (medianPFC =  $6.3^\circ$ , medianVIP =  $7.5^\circ$ ; two-sided Mann–Whitney test,  $Z = -3.18$ ,  $P = 0.002$ ).

#### Receptive fields properties by neuron types

As different neuronal subtypes might well exhibit characteristically different receptive fields, we sorted the recorded neurons into putatively pyramidal (broad-spiking, BS) and interneuron (narrow-spiking, NS) classes based on their waveform widths (Fig. 8A and B; Swadlow & Weyand, 1987; Constantinidis & Goldman-Rakic, 2002; Diester & Nieder, 2008; Viswanathan & Nieder, 2015, 2017).

In terms of RF eccentricity, both BS neurons and NS neurons in dIPFC displayed similar eccentricities (Fig. 8C). Median BS neurons had fields located  $11.9^\circ$  from the centre and median NS neurons at  $12.4^\circ$  (Mann–Whitney *U*-test,  $Z = 0.58$ ,  $P = 0.56$ ). This was also the case for VIP eccentricities (Fig. 8D). BS neurons had a median eccentricity of  $11.2^\circ$  and NS neurons,  $9.1^\circ$  (Mann–Whitney *U*-test,  $Z = 0.86$ ,  $P = 0.39$ ).

When comparing sizes of screen-limited RFs within dIPFC, we found that BS neurons displayed smaller RFs than NS neurons (Fig. 8E). BS neurons had receptive fields of a median  $6.1^\circ$  and NS neurons,  $8.7^\circ$  (Mann–Whitney *U*-test,  $Z = -2.33$ ,  $P = 0.02$ ). In VIP, however, we found no significant differences between the two neuronal classes in field size (Fig. 8F). Both BS neurons and NS neurons had a median RF size between  $7.2^\circ$  and  $8.3^\circ$  (Mann–Whitney *U*-test,  $Z = -1.81$ ,  $P = 0.07$ ).

#### Discussion

While monkeys fixated passively, we found that more than half of the recorded dIPFC and VIP neurons responded selectively to a moving bar presented at various locations of the screen. VIP neurons displayed larger RFs that were more foveally located than PFC receptive fields, which were more contralateral. Additionally, VIP neurons were more strongly modulated by position than PFC neurons. Finally, putative inhibitory neurons in PFC displayed larger RFs than excitatory neurons but across the same eccentricities while no such difference was seen across VIP neuronal classes.

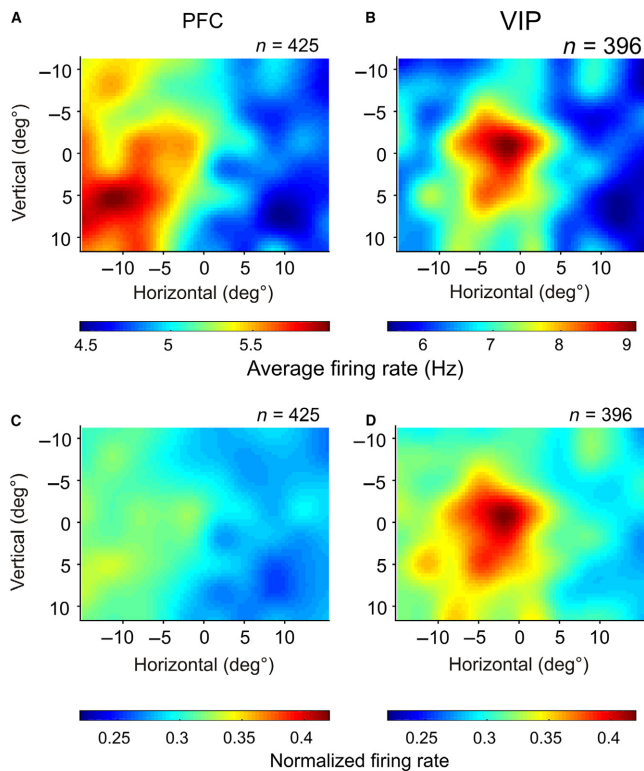


FIG. 4. Average RF maps. (A) Average of all 425 PFC RF maps as a heat map. The average firing rate is shown in the colour bar below. (B) Average of all 396 VIP RF maps. (C) Average of all PFC maps normalised individually to their maxima. The normalised firing rate is shown in the colour bar below. (D) the same as C for all VIP RFs. VIP neurons show higher spatial modulation. [Colour figure can be viewed at [wileyonlinelibrary.com](http://wileyonlinelibrary.com)].

#### Visual RFs in dIPFC and VIP during passive fixation

Our study represents the most detailed characterisation of receptive fields in dorsolateral prefrontal cortex (dIPFC) and VIP, not only in the number of neurons sampled, but also in the resolution of mapping, that is 80 positions across  $30.5^\circ$  (horizontal)  $\times$   $23^\circ$  (vertical) of the visual field. As a result, a majority of cells in dIPFC and VIP could be activated to construct high-resolution spatial RF maps. Bar stimuli with a higher range of sizes, speeds and directions (Schaafsma & Duysens, 1996; Bremmer *et al.*, 2002; Gabel *et al.*, 2002) might have activated even more neurons. Moreover, probabilistic mapping has been proposed as an efficient method to assess the spatio-temporal structures of frontal eye field (FEF) receptive fields (Mayo *et al.*, 2015, 2016).

One of the prime problems in RF mappings therefore, is that of the optimal stimulus to be used. This is a relatively simple issue for early visual areas, but a graver problem higher up the processing hierarchy. After all, neurons in the association cortices process higher-order information pertinent to all sorts of cognitive processing. The dIPFC, in particular, is a high-level area that is operating at the apex of the cortical hierarchy and is renowned for encoding highly cognitive parameters, such as perceptual categories (Freedman & Assad, 2016), numerical quantities (Nieder *et al.*, 2002; Nieder, 2012; Viswanathan & Nieder, 2013; Ramirez-Cardenas *et al.*, 2016), rules (Bongard & Nieder, 2010; Eisele & Nieder, 2013; Ott *et al.*, 2014), reward contingencies (Kennerley & Wallis, 2009; Asaad & Eskandar, 2011) and other behavioural principles. But also VIP neurons operating slightly more upstream of the cortical hierarchy are well known to represent almost equally abstract concepts

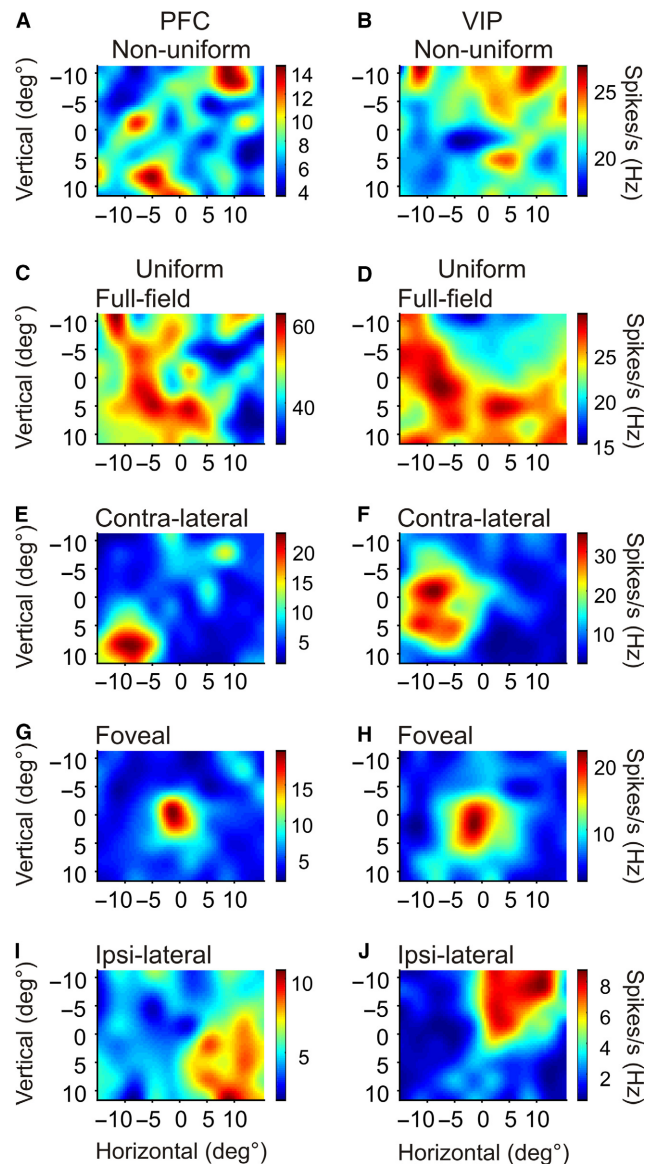


FIG. 5. Characterisation of RF types. Examples of receptive field types from PFC (left column) and VIP (right column), presented as RF maps with the colours indicating individual firing rates. (A and B) Non-uniform receptive field showing  $>1$  discrete locations with maximal response. (C–J) Uniform receptive fields consisting of subtypes. (C and D) Full-field responses with more than 75% of locations with  $>$ half-max responses. (E–J) Uniform, confined responses. (E and F) Contralateral receptive fields with the RF maxima situated on the contralateral third of the screen. (G and H) Foveal receptive fields covering the central portion of the screen. (I and J) Ipsilateral receptive fields with the maxima situated ipsilaterally. [Colour figure can be viewed at [wileyonlinelibrary.com](http://wileyonlinelibrary.com)].

(Tudusciuc & Nieder, 2009; Nieder, 2012; Jacob & Nieder, 2014). As both VIP and dIPFC require sensory input, tuning to simple stimuli must emerge due to visual input from upstream visual areas where neurons respond to basic features. Despite the anatomical and functional distance of VIP and dIPFC from the early visual areas, it is surprising to find confined visual responses to basic visual parameters in these association cortices. As visual RFs in the association cortices are indicative of default anatomical wiring, this default wiring might be useful for multi-modal integration and the mapping of different reference frames onto a circuit.

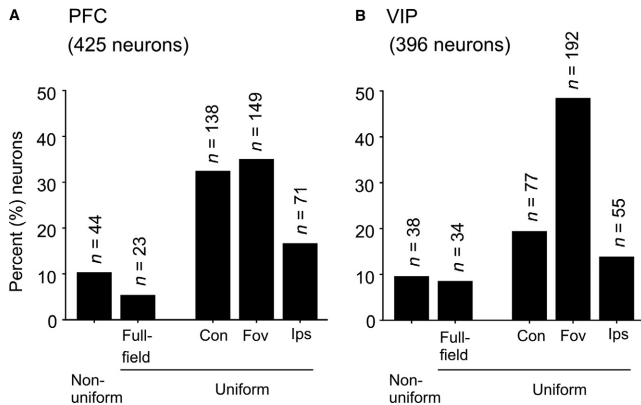


FIG. 6. Frequencies of different RF types. (A) Percentage of neurons that exhibit various types of receptive fields in PFC, (B) and VIP. The number of neurons in each case is indicated above the bar. The frequency of non-uniform and uniform RFs is similar in both areas. The contralateral, foveal and ipsilateral RFs constitute the uniform, confined population. PFC contains more contralateral RFs than VIP and VIP more foveal RFs.

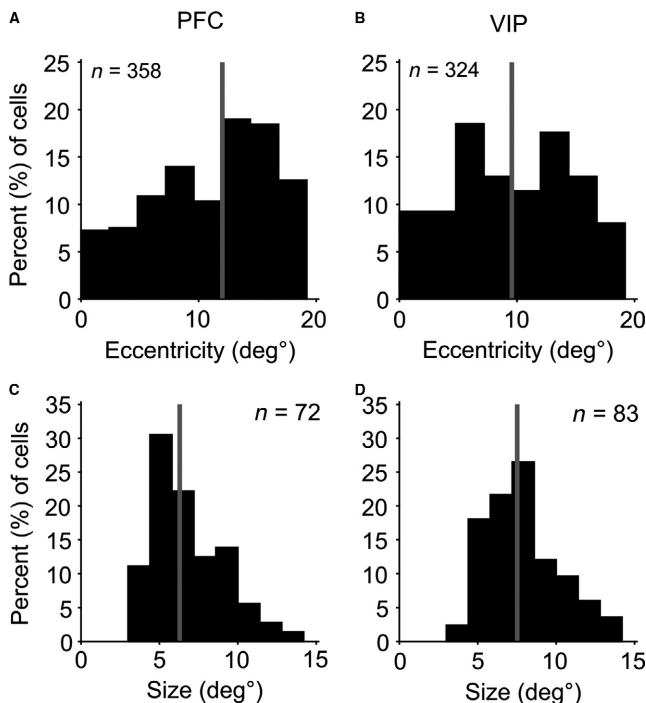


FIG. 7. Receptive field properties of confined RFs (A) Probability histograms of eccentricity measured in degrees of visual angle from the centre, for uniform, confined RFs in PFC, (B) and VIP. Vertical grey lines mark the medians of the distributions. (C) Histogram of PFC receptive field sizes, in dva, of neurons whose fields were uniform, confined and did not touch the borders of the screen (screen-limited). These could, thus, be reliably measured in our experiment. (D) the same as C for VIP neurons.

In the case of dIPFC, early studies reported confined visual responses (Mikami *et al.*, 1982; Suzuki & Azuma, 1983). Neurons around the principal sulcus were responsive to a moving slit/dot presented foveally or para-foveally. The visual receptive fields in dIPFC thus recorded were found to be largely contralateral and in strong agreement with our data though less was reported about their spatial structure than the latency of their responses. Neurons rostral to the inferior arcuate sulcus were said to have small, foveal RFs and those in the anterior and posterior parts of the prearcuate area had large

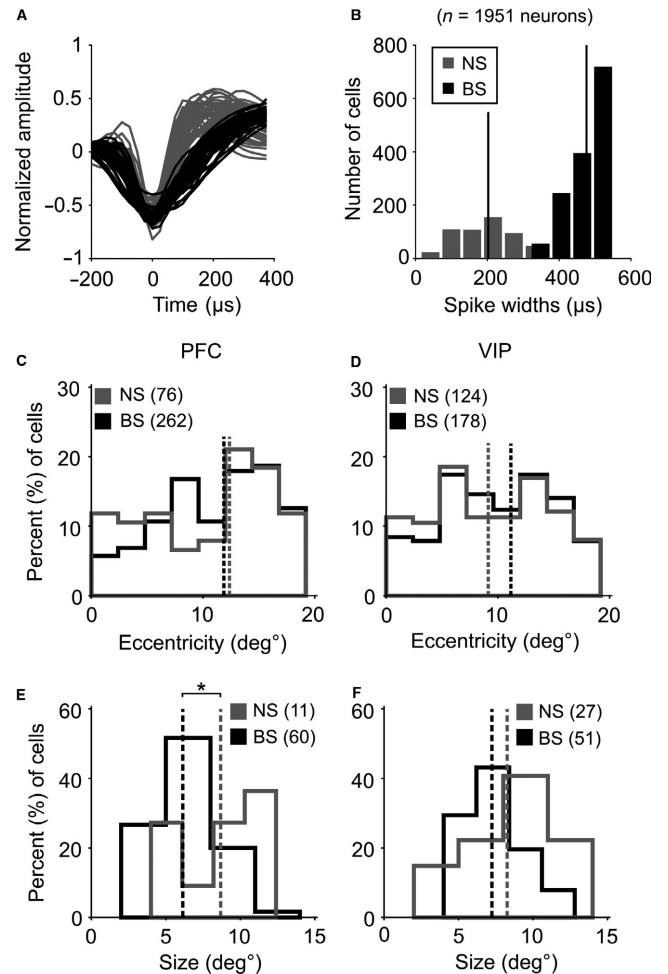


FIG. 8. Receptive field properties by neuron class (A) Classification of neuronal classes by waveforms; 50 randomly chosen narrow-spiking (NS) neurons are shown in grey, and broad-spiking (BS) neurons in black. The waveforms are normalised and aligned to their troughs. (B) Histogram of spike widths for all NS and BS neurons with the means of both classes plotted as black vertical lines. (C) Probability histograms of RF eccentricity by neuron class in PFC, (D) in VIP. The vertical lines mark the medians of the respective distributions. (E) Probability histograms of RF sizes by neuron class in PFC, (F) and VIP. Dotted vertical lines mark the medians of the RF sizes. PFC BS neurons had smaller RFs than NS neurons (Mann–Whitney *U*-test,  $P = 0.02$ ).

RFs at greater eccentricities (Suzuki & Azuma, 1983; Riley *et al.*, 2017). We did not find such a reliable layout of dIPFC RFs based on our small number of recording sites.

Much more is known about the receptive fields in VIP, which is part of the cluster of IPS areas that constitute the termination zone of the dorsal, parietal visual stream (Mishkin *et al.*, 1983). For instance, RFs of many VIP neurons are not only visual, but multi-modal (Bremner *et al.*, 2002; Schlack *et al.*, 2005), and show shifts according to different frames of reference (Chen *et al.*, 2011, 2014). Still, the size and eccentricity of these fields within a retinotopic frame were unknown. These features of the receptive field are important as clues to function. For instance, lateral intraparietal area (LIP) receptive fields, on average, fall a bit eccentric from the fovea at about  $5^\circ$  (Janssen *et al.*, 2008) while posterior anterior intraparietal area (pAIP) receptive fields are frequently foveal (Romero & Janssen, 2016). It has been proposed that this difference reflects the role of LIP in saccade movements and of pAIP in grasping as objects are often foveated before successful grasping (Blatt *et al.*, 1990; Ben Hamed *et al.*,

2001). VIP receptive fields in our study are much more reminiscent of AIP RFs than those of LIP in their spans and possibly reflect the role of VIP in multi-sensory integration and transformations (Bremmer *et al.*, 2002; Schlack *et al.*, 2005; Zhang & Britten, 2011).

### *From passive to active vision*

The dIPFC and VIP are part of the frontal and parietal association cortices, respectively. As such, they show non-canonical circuit properties characteristic of the association cortices (Goldman-Rakic, 1988). Non-canonical circuits enable parallel and re-entrant processing required for persistent activity shown by PFC and PPC neurons during temporal delays in cognitive task. Because of this functionality, neurons in the association cortices are expected to be released from the rigid topographic layout found in early sensory areas (Galletti *et al.*, 1999). Indeed, we have recently demonstrated that neurons in dIPFC and VIP show progressively lower spatiotopy than has been reported for neurons in early visual cortices (Viswanathan & Nieder, 2017), dIPFC much less than VIP. Pairs of neurons recorded at the same electrode tip often had dissimilar or inverted RFs, contrary to the more than 80% spatial similarity seen in neighbouring RFs in early visual cortices (Das & Gilbert, 1997; DeAngelis *et al.*, 1999).

Unlike neurons in early visual areas that have to provide a veridical representation of the outside world, neurons in the association cortices are more related to the internal state of an animal. Therefore, spatial visual representations may become modulated or changed by cognitive factors, such as spatial attention or the grouping of objects into behaviourally meaningful categories. Indeed, they have been found to shift sometimes dramatically with behavioural relevance in active tasks (Freedman & Assad, 2006; Viswanathan & Nieder, 2015). When active tasks involve the discrimination of spatial features, PFC neurons encode the location of an object along with its identity during a matching task (Funahashi & Bruce, 1989; Rainer *et al.*, 1998a), or differentially encode the location of an object based on the ongoing task (Asaad *et al.*, 2000). PFC neurons also shift the response field with attention and filter out spatial locations that are unattended (Everling *et al.*, 2002) or non-target (Rainer *et al.*, 1998b). We know that even working memory activity in PFC is shaped by the identity of the object as by the location of the object (Rainer *et al.*, 1998a; Kennerly & Wallis, 2009).

Areas in the parietal cortex have been mapped in tasks involving saccades (Dunn & Colby, 2010) to ensure strong neuronal responses at the visual location being tested (Colby *et al.*, 1996). VIP neurons also exhibit strong modulation by attentional signals (Cook & Maunsell, 2002). It may therefore be expected that visual RFs in the association cortex shift and change with cognitive demands (Ben Hamed *et al.*, 2002; Womelsdorf *et al.*, 2008). Further research would be required to show the potential flexibility of these maps during active spatial discrimination, or whether the receptive field structures and locations play a role when the animals are involved in a non-spatial task (Freedman & Assad, 2009; Ibos & Freedman, 2016). An ongoing task might recruit spatially selective neurons in non-spatial events. As we find VIP neurons to be more strongly modulated by space than PFC neurons, we predict that VIP neurons would be weakly recruited when stimuli are presented outside of their RFs, whereas PFC neurons would be more independent from their passive, default RFs.

### *Pyramidal neurons and interneurons*

Pyramidal neurons and interneurons, the two major cell classes in the neocortex, sculpt neuronal response properties in different

contexts. We have observed that putative pyramidal neurons in PFC showed increased modulation by the behaviourally relevant numerosity stimuli than interneurons (Viswanathan & Nieder, 2015). Several other studies suggest differential participation of prefrontal pyramidal neurons and interneurons in behavioural relevance (Hussar & Pasternak, 2009), in working memory (Hussar & Pasternak, 2012) and in learned numerosity representations (Diester & Nieder, 2008). Putative pyramidal neurons exhibit sharper tuning and stable representations of features while interneurons facilitate flexibility by responding strongly to changes in context or task demands. These differences together with the observed difference in RF sizes indicate that these neuronal classes are set up for differential recruitment by their circuitry. Our finding of larger RFs in PFC interneurons might enable them to participate more flexibly in active tasks whereas smaller RFs in pyramidal neurons allow them to sharply distinguish stimulus features. This is supported by the finding that putative pyramidal neurons in area LIP were selective to fine features of the stimuli whereas interneurons responded strongly to target stimuli and were not as selective for the finer stimulus features (Yokoi & Komatsu, 2010). Differential targeting by different interneuron subtypes shaped persistent activity in PFC pyramidal neurons and lends weight to the idea of distributed roles in spatial tuning (Wang *et al.*, 2004). Spatial tuning in dIPFC is significantly impaired with iontophoretic disinhibition (Rao *et al.*, 2000). PFC interneurons, while similarly tuned (to similar eccentricities) as pyramidal neurons during sensory and delay phases shifted their tuning in response phases to opposite directions, exhibiting greater flexibility than pyramidal neurons (Rao *et al.*, 1999). VIP neurons, whose RFs do not show a difference in sizes or eccentricities for the two neuronal classes, might share their task loads more equitably.

Understanding how different neuronal classes participate in such circuitry and how they represent visual space are important steps in understanding how our visual space might be represented in cortical circuits. Together with our recent results about the non-canonical arrangement about RFs in association cortices, we suggest that RFs of sensory neurons may play very different roles according to where in the processing streams they lie.

### Acknowledgements

This work was supported by DFG grant NI 618/2-1 to A.N.

### Conflict of interest

The authors declare no competing financial interests.

### Author contributions

P.V. and A.N. designed research; P.V. performed research; P.V. and A.N. wrote the paper.

### Data accessibility

All primary data generated in this study will be available upon request.

### Abbreviations

AIP, anterior intraparietal area; ANOVA, analysis of variance; BS, broad-spiking neurons; cdf, cumulative distribution function; dIPFC, dorsolateral prefrontal cortex; FEF, frontal eye field; IPS, intraparietal sulcus; LIP, lateral intraparietal area; LS, lateral sulcus; MRI, magnetic resonance imaging; MT,

middle temporal area; NS, narrow-spiking neurons; pAIP, posterior anterior intraparietal area; PFC, prefrontal cortex; PPC, posterior parietal cortex; PS, principal sulcus; RF, receptive field; STS, superior temporal sulcus; VIP, ventral intraparietal area;  $\omega^2$ , omega-squared (measure of effect size).

## References

- Alonso, J.-M. (2002) Neural connections and receptive field properties in the primary visual cortex. *Neuroscientist*, **8**, 443–456.
- Asaad, W.F. & Eskandar, E.N. (2011) Encoding of both positive and negative reward prediction errors by neurons of the primate lateral prefrontal cortex and caudate nucleus. *J. Neurosci.*, **31**, 17772–17787.
- Asaad, W.F., Rainer, G. & Miller, E.K. (2000) Task-specific neural activity in the primate prefrontal cortex. *J. Neurophysiol.*, **84**, 451–459.
- Avillac, M., Denève, S., Olivier, E., Pouget, A. & Duhamel, J.-R. (2005) Reference frames for representing visual and tactile locations in parietal cortex. *Nat. Neurosci.*, **8**, 941–949.
- Avillac, M., Ben Hamed, S. & Duhamel, J.-R. (2007) Multisensory integration in the ventral intraparietal area of the macaque monkey. *J. Neurosci.*, **27**, 1922–1932.
- Ben Hamed, S., Duhamel, J.R., Bremmer, F. & Graf, W. (2001) Representation of the visual field in the lateral intraparietal area of macaque monkeys: a quantitative receptive field analysis. *Exp. Brain Res.*, **140**, 127–144.
- Ben Hamed, S., Duhamel, J.-R., Bremmer, F. & Graf, W. (2002) Visual receptive field modulation in the lateral intraparietal area during attentive fixation and free gaze. *Cereb. Cortex*, **12**, 234–245.
- Blatt, G.J., Andersen, R.A. & Stoner, G.R. (1990) Visual receptive field organization and cortico-cortical connections of the lateral intraparietal area (area LIP) in the macaque. *J. Comp. Neurol.*, **299**, 421–445.
- Bongard, S. & Nieder, A. (2010) Basic mathematical rules are encoded by primate prefrontal cortex neurons. *P. Natl. Acad. Sci. USA*, **107**, 2277–2282.
- Bremmer, F. (2011) Multisensory space: from eye-movements to self-motion. *J. Physiol.*, **589**, 815–823.
- Bremmer, F., Klam, F., Duhamel, J.-R., Ben Hamed, S. & Graf, W. (2002) Visual-vestibular interactive responses in the macaque ventral intraparietal area (VIP). *Eur. J. Neurosci.*, **16**, 1569–1586.
- Buschman, T.J. & Miller, E.K. (2007) Top-down versus bottom-up control of attention in the prefrontal and posterior parietal cortices. *Science*, **315**, 1860–1862.
- Chafee, M.V. & Goldman-Rakic, P.S. (2000) Inactivation of parietal and prefrontal cortex reveals interdependence of neural activity during memory-guided saccades. *J. Neurophysiol.*, **83**, 1550–1566.
- Chen, A., DeAngelis, G.C. & Angelaki, D.E. (2011) A comparison of vestibular spatiotemporal tuning in macaque parietoinsular vestibular cortex, ventral intraparietal area, and medial superior temporal area. *J. Neurosci.*, **31**, 3082–3094.
- Chen, X., DeAngelis, G.C. & Angelaki, D.E. (2014) Eye-centered visual receptive fields in the ventral intraparietal area. *J. Neurophysiol.*, **112**, 353–361.
- Colby, C.L., Duhamel, J.R. & Goldberg, M.E. (1993) Ventral intraparietal area of the macaque: anatomic location and visual response properties. *J. Neurophysiol.*, **69**, 902–914.
- Colby, C.L., Duhamel, J.R. & Goldberg, M.E. (1996) Visual, presaccadic, and cognitive activation of single neurons in monkey lateral intraparietal area. *J. Neurophysiol.*, **76**, 2841–2852.
- Constantinidis, C. & Goldman-Rakic, P.S. (2002) Correlated discharges among putative pyramidal neurons and interneurons in the primate prefrontal cortex. *J. Neurophysiol.*, **88**, 3487–3497.
- Cook, E.P. & Maunsell, J.H.R. (2002) Attentional modulation of behavioral performance and neuronal responses in middle temporal and ventral intraparietal areas of macaque monkey. *J. Neurosci.*, **22**, 1994–2004.
- Crowe, D.A., Goodwin, S.J., Blackman, R.K., Sakellaridi, S., Sponheim, S.R., MacDonald, A.W. & Chafee, M.V. (2013) Prefrontal neurons transmit signals to parietal neurons that reflect executive control of cognition. *Nat. Neurosci.*, **16**, 1484–1491.
- Das, A. & Gilbert, C.D. (1997) Distortions of visuotopic map match orientation singularities in primary visual cortex. *Nature*, **387**, 594–598.
- DeAngelis, G.C., Ghose, G.M., Ohzawa, I. & Freeman, R.D. (1999) Functional micro-organization of primary visual cortex: receptive field analysis of nearby neurons. *J. Neurosci.*, **19**, 4046–4064.
- Diester, I. & Nieder, A. (2008) Complementary contributions of prefrontal neuron classes in abstract numerical categorization. *J. Neurosci.*, **28**, 7737–7747.
- Duhamel, J.-R.R., Bremmer, F., Ben Hamed, S. & Graf, W. (1997) Spatial invariance of visual receptive fields in parietal cortex neurons. *Nature*, **389**, 845–848.
- Dunn, C.A. & Colby, C.L. (2010) Representation of the ipsilateral visual field by neurons in the macaque lateral intraparietal cortex depends on the forebrain commissures. *J. Neurophysiol.*, **104**, 2624–2633.
- Eiselt, A.-K. & Nieder, A. (2013) Representation of abstract quantitative rules applied to spatial and numerical magnitudes in primate prefrontal cortex. *J. Neurosci.*, **33**, 7526–7534.
- Everling, S., Tinsley, C.J., Gaffan, D. & Duncan, J. (2002) Filtering of neural signals by focused attention in the monkey prefrontal cortex. *Nat. Neurosci.*, **5**, 671–676.
- Freedman, D.J. & Assad, J.A. (2006) Experience-dependent representation of visual categories in parietal cortex. *Nature*, **443**, 85–88.
- Freedman, D.J. & Assad, J.A. (2009) Distinct encoding of spatial and non-spatial visual information in parietal cortex. *J. Neurosci.*, **29**, 5671–5680.
- Freedman, D.J. & Assad, J.A. (2016) Neuronal mechanisms of visual categorization: an abstract view on decision making. *Annu. Rev. Neurosci.*, **39**, 129–147.
- Funahashi, S. & Bruce, C.J. (1989) Mnemonic coding of visual space in the monkey's dorsolateral prefrontal cortex. *J. Neurophysiol.*, **61**, 331–349.
- Fuster, J.M. & Alexander, G.E. (1971) Neuron activity related to short-term memory. *Science*, **173**, 652–654.
- Fuster, J.M. & Bauer, R.H. (1974) Visual short-term memory deficit from hypothermia of frontal cortex. *Brain Res.*, **81**, 393–400.
- Gabel, S.F., Misslisch, H., Schaafsma, S.J. & Duysens, J. (2002) Temporal properties of optic flow responses in the ventral intraparietal area. *Vis. Neurosci.*, **19**, 381–388.
- Galletti, C., Fattori, P., Gamberini, M. & Kutz, D.F. (1999) The cortical visual area V6: brain location and visual topography. *Eur. J. Neurosci.*, **11**, 3922–3936.
- Goldman-Rakic, P.S. (1988) Topography of cognition: parallel distributed networks in primate association cortex. *Annu. Rev. Neurosci.*, **11**, 137–156.
- Hubel, D.H. & Wiesel, T.N. (1962) Receptive fields, binocular interaction and functional architecture in the cat's visual cortex. *J. Physiol.*, **160**, 106–154.
- Hussar, C.R. & Pasternak, T. (2009) Flexibility of sensory representations in prefrontal cortex depends on cell type. *Neuron*, **64**, 730–743.
- Hussar, C.R. & Pasternak, T. (2012) Memory-guided sensory comparisons in the prefrontal cortex: contribution of putative pyramidal cells and interneurons. *J. Neurosci.*, **32**, 2747–2761.
- Ibos, G. & Freedman, D.J. (2016) Interaction between spatial and feature attention in posterior parietal cortex. *Neuron*, **91**, 931–943.
- Jacob, S.N. & Nieder, A. (2014) Complementary roles for primate frontal and parietal cortex in guarding working memory from distractor stimuli. *Neuron*, **83**, 226–237.
- Janssen, P., Srivastava, S., Ombelet, S. & Orban, G.A. (2008) Coding of shape and position in macaque lateral intraparietal area. *J. Neurosci.*, **28**, 6679–6690.
- Kennerley, S.W. & Wallis, J.D. (2009) Encoding of reward and space during a working memory task in the orbitofrontal cortex and anterior cingulate sulcus. *J. Neurophysiol.*, **102**, 3352–3364.
- Lewis, J.W. & Van Essen, D.C. (2000) Corticocortical connections of visual, sensorimotor, and multimodal processing areas in the parietal lobe of the macaque monkey. *J. Comp. Neurol.*, **428**, 112–137.
- Mayo, J.P., DiTomasso, A.R., Sommer, M.A. & Smith, M.A. (2015) Dynamics of visual receptive fields in the macaque frontal eye field. *J. Neurophysiol.*, **114**, 3201–3210.
- Mayo, J.P., Morrison, R.M. & Smith, M.A. (2016) A probabilistic approach to receptive field mapping in the frontal eye fields. *Front. Syst. Neurosci.*, **10**, 25.
- Mikami, A., Ito, S. & Kubota, K. (1982) Visual response properties of dorso-lateral prefrontal neurons during visual fixation task. *J. Neurophysiol.*, **47**, 593–605.
- Mishkin, M., Ungerleider, L.G. & Macko, K.A. (1983) Object vision and spatial vision: two cortical pathways. *Trends Neurosci.*, **6**, 414–417.
- Nieder, A. (2012) Supramodal numerosity selectivity of neurons in primate prefrontal and posterior parietal cortices. *P. Natl. Acad. Sci. USA*, **109**, 11860–11865.
- Nieder, A. (2016) The neuronal code for number. *Nat. Rev. Neurosci.*, **17**, 366–382.
- Nieder, A. & Miller, E.K. (2004) A parieto-frontal network for visual numerical information in the monkey. *P. Natl. Acad. Sci. USA*, **101**, 7457–7462.
- Nieder, A., Freedman, D.J. & Miller, E.K. (2002) Representation of the quantity of visual items in the primate prefrontal cortex. *Science*, **297**, 1708–1711.
- Ott, T., Jacob, S.N. & Nieder, A. (2014) Dopamine receptors differentially enhance rule coding in primate prefrontal cortex neurons. *Neuron*, **84**, 1317–1328.

- Pandya, D.N. & Yeterian, E.H. (1991) Chapter 4 Prefrontal cortex in relation to other cortical areas in rhesus monkey: architecture and connections. *Prog. Brain Res.*, **85**, 63–94.
- Quintana, J. & Fuster, J.M. (1999) From perception to action: temporal integrative functions of prefrontal and parietal neurons. *Cereb. Cortex*, **9**, 213–221.
- Rainer, G., Asaad, W.F. & Miller, E.K. (1998a) Memory fields of neurons in the primate prefrontal cortex. *P. Natl. Acad. Sci. USA*, **95**, 15008–15013.
- Rainer, G., Asaad, W.F. & Miller, E.K. (1998b) Selective representation of relevant information by neurons in the primate prefrontal cortex. *Nature*, **393**, 577–579.
- Ramirez-Cardenas, A., Moskaleva, M. & Nieder, A. (2016) Neuronal representation of numerosity zero in the primate parieto-frontal number network. *Curr. Biol.*, **26**, 1285–1294.
- Rao, S.G., Williams, G.V. & Goldman-Rakic, P.S. (1999) Isodirectional tuning of adjacent interneurons and pyramidal cells during working memory: evidence for microcolumnar organization in PFC. *J. Neurophysiol.*, **81**, 1903–1916.
- Rao, S.G., Williams, G.V. & Goldman-Rakic, P.S. (2000) Destruction and creation of spatial tuning by disinhibition: GABA(A) blockade of prefrontal cortical neurons engaged by working memory. *J. Neurosci.*, **20**, 485–494.
- Riley, M.R., Qi, X.-L. & Constantinidis, C. (2017) Functional specialization of areas along the anterior-posterior axis of the primate prefrontal cortex. *Cereb. Cortex*, **27**, 3683–3697.
- Romero, M.C. & Janssen, P. (2016) Receptive field properties of neurons in the macaque anterior intraparietal area. *J. Neurophysiol.*, **115**, 1542–1555.
- Romo, R., Brody, C.D., Hernández, A. & Lemus, L. (1999) Neuronal correlates of parametric working memory in the prefrontal cortex. *Nature*, **399**, 470–473.
- Schaafsma, S.J. & Duysens, J. (1996) Neurons in the ventral intraparietal area of awake macaque monkey closely resemble neurons in the dorsal part of the medial superior temporal area in their responses to optic flow patterns. *J. Neurophysiol.*, **76**, 4056–4068.
- Schlack, A., Sterbing-D'Angelo, S.J., Hartung, K., Hoffmann, K.-P. & Bremner, F. (2005) Multisensory space representations in the macaque ventral intraparietal area. *J. Neurosci.*, **25**, 4616–4625.
- Schwartz, M.L. & Goldman-Rakic, P.S. (1984) Callosal and intrahemispheric connectivity of the prefrontal association cortex in rhesus monkey: relation between intraparietal and principal sulcal cortex. *J. Comp. Neurol.*, **226**, 403–420.
- Solomon, S.G., White, A.J.R. & Martin, P.R. (2002) Extraclassical receptive field properties of parvocellular, magnocellular, and koniocellular cells in the primate lateral geniculate nucleus. *J. Neurosci.*, **22**, 338–349.
- Sugihara, T., Diltz, M.D., Averbek, B.B. & Romanski, L.M. (2006) Integration of auditory and visual communication information in the primate ventrolateral prefrontal cortex. *J. Neurosci.*, **26**, 11138–11147.
- Suzuki, H. (1985) Distribution and organization of visual and auditory neurons in the monkey prefrontal cortex. *Vision Res.*, **25**, 465–469.
- Suzuki, H. & Azuma, M. (1983) Topographic studies on visual neurons in the dorsolateral prefrontal cortex of the monkey. *Exp. Brain Res.*, **53**, 47–58.
- Swadlow, H.A. & Gusev, A.G. (2002) Receptive-field construction in cortical inhibitory interneurons. *Nat. Neurosci.*, **5**, 403–404.
- Swadlow, H.A. & Weyand, T.G. (1987) Corticogeniculate neurons, corticotectal neurons, and suspected interneurons in visual cortex of awake rabbits: receptive-field properties, axonal properties, and effects of EEG arousal. *J. Neurophysiol.*, **57**, 977–1001.
- Swaminathan, S.K. & Freedman, D.J. (2012) Preferential encoding of visual categories in parietal cortex compared with prefrontal cortex. *Nat. Neurosci.*, **15**, 315–320.
- Tudusciuc, O. & Nieder, A. (2009) Contributions of primate prefrontal and posterior parietal cortices to length and numerosity representation. *J. Neurophysiol.*, **101**, 2984–2994.
- Vallentin, D., Bongard, S. & Nieder, A. (2012) Numerical rule coding in the prefrontal, premotor, and posterior parietal cortices of macaques. *J. Neurosci.*, **32**, 6621–6630.
- Veit, J., Bhattacharyya, A., Kretz, R. & Rainer, G. (2014) On the relation between receptive field structure and stimulus selectivity in the tree shrew primary visual cortex. *Cereb. Cortex*, **24**, 2761–2771.
- Viswanathan, P. & Nieder, A. (2013) Neuronal correlates of a visual “sense of number” in primate parietal and prefrontal cortices. *P. Natl. Acad. Sci. USA*, **110**, 11187–11192.
- Viswanathan, P. & Nieder, A. (2015) Differential impact of behavioral relevance on quantity coding in primate frontal and parietal neurons. *Curr. Biol.*, **25**, 1259–1269.
- Viswanathan, P. & Nieder, A. (2017) Visual receptive field heterogeneity and functional connectivity of adjacent neurons in primate fronto-parietal association cortices. *J. Neurosci.*, **37**, 8919–8928.
- Wang, X.-J., Tegnér, J., Constantinidis, C. & Goldman-Rakic, P.S. (2004) Division of labor among distinct subtypes of inhibitory neurons in a cortical microcircuit of working memory. *P. Natl. Acad. Sci. USA*, **101**, 1368–1373.
- Wang, L., Li, X., Hsiao, S.S., Lenz, F.A., Bodner, M., Zhou, Y.-D. & Fuster, J.M. (2015) Differential roles of delay-period neural activity in the monkey dorsolateral prefrontal cortex in visual-haptic crossmodal working memory. *P. Natl. Acad. Sci. USA*, **112**, E214–E219.
- Womelsdorf, T., Anton-Erxleben, K. & Treue, S. (2008) Receptive field shift and shrinkage in macaque middle temporal area through attentional gain modulation. *J. Neurosci.*, **28**, 8934–8944.
- Yokoi, I. & Komatsu, H. (2010) Putative pyramidal neurons and interneurons in the monkey parietal cortex make different contributions to the performance of a visual grouping task. *J. Neurophysiol.*, **104**, 1603–1611.
- Yoshor, D., Bosking, W.H., Ghose, G.M. & Maunsell, J.H.R. (2007) Receptive fields in human visual cortex mapped with surface electrodes. *Cereb. Cortex*, **17**, 2293–2302.
- Zhang, T. & Britten, K.H. (2011) Parietal area VIP causally influences heading perception during pursuit eye movements. *J. Neurosci.*, **31**, 2569–2575.